AN INCREMENTAL MODAL SHAPE SENSING METHOD FOR GEOMETRICALLY NON-LINEAR DEFORMED WINGS

Janto Gundlach[1], **Marc Böswald**[1], **Jurij Sodja**[2]

[1]German Aerospace Center
Bunsenstraße 10, 37073 Göttingen, Germany
janto.gundlach@dlr.de
marc.boeswald@dlr.de

[2]Delft University of Technology
Kluyverweg 1, 2629HS Delft, The Netherlands
j.sodja@tudelft.nl

Keywords: Shape sensing, mode shapes, modal approach, large deformation, geometric non-linearity

Abstract: Shape sensing techniques enable the real-time reconstruction of wing displacements based on measured strain. As wing designs become more flexible, they may at some point exhibit geometric non-linear deformation. This eventually leads to erroneous displacement estimates if applied methods rely on the assumption of linear deformation. In this research, the Incremental Modal Method (IMM) is presented which accounts for the change of the employed mode shapes due to structural deformation. The method is applied on the finite element model of a high aspect ratio wing undergoing geometric non-linear deflections in flap-wise bending. In the process, a setup of virtual strain sensors is presumed which is representative as instrumentation in experiments. Along a reference line of the wing, the displacement estimates of IMM are compared to results obtained using the Modal Rotation Method (MRM), another shape sensing scheme recently developed for the non-linear regime. For the chosen segmentation and virtual instrumentation of the investigated wing, IMM proves to be a promising candidate for real-time displacement reconstruction in experiments, provided that mode shapes in intermediate deflected states can be determined.

1 INTRODUCTION

The displacement reconstruction of wing-like structures based on strain, commonly referred to as shape sensing, is a prospective method for monitoring the state of deformation whenever a direct measurement is not feasible. A large number of methods have been established and the majority of available techniques can be categorised in three different groups: methods exploiting the kinematics of structural elements such as beams [1], methods minimising error functionals in the framework of inverse finite elements [2], and methods that linearly superpose basis functions to reconstruct displacements [3,4]. These methods all have in common that they only allow displacement predictions for linear deformations of the structure.
An observed trend in aircraft design to reduce lift-induced drag is to increase wing aspect ratio. As wings with longer spans are more susceptible to large deflections, their aeroelastic behavior is prone to being influenced by geometric non-linearities. In this context, the source of non-linearity is classified geometric if changes of the system behaviour are caused by significant alteration of the geometry with respect to its initial state. Such non-linear behaviour may occur

as gust or manoeuvre load response, but it can already be encountered in cruise conditions of very flexible aerial vehicles [5]. The aforementioned traditional shape sensing methods applied on such problems lead to erroneous assessment of the deformation. To overcome this issue, new approaches tailored specifically to geometric non-linearity have been presented recently, where either modal rotations [6, 7] or static non-linear deflection curves [8] of the structure are used for the deformation reconstruction. These prerequisites are derived from a Finite Element (FE) model of the structure.

Among other flight dynamic scenarios, in both flight and wind tunnel tests, data is collected at stationary test points within the test envelope. These test points serve as linearisation points to determine the modal parameters of the aeroelastic system and to assess flutter stability [9]. For flexible wings, different test points are typically associated to different states of deflection. Following the idea of [10], it may thus be prospective to exploit methods that have been developed for linear deformation in an incremental sense also for the geometrically non-linear regime. In this way, the deformation reconstruction could be accomplished solely based on measured quantities.

In the present research a shape sensing method belonging to the third mentioned category, using mode shapes as basis functions (cf. [3, 11]), is extended to incremental use. Employing mode shapes in a linear combination for displacement reconstruction is particularly fruitful, since this fulfils the modal approach. In contrast to the original method, the proposed technique utilises strain and displacement mode shapes determined in different states of deformation. In the context of an aeroelastic experiment, the stationary points of the test envelope represent these states, which are connected to each other in an incremental procedure in order to achieve deformations in the geometrically non-linear regime. The method is therefore denoted Incremental Modal Method (IMM).

In order to demonstrate the above described process, IMM is applied to simulation results of an FE model of a test wing undergoing large deflections. The wing is intended to be used for validation of the method in future experiments. On that account, strain data is considered at positions on the wing which are representative as test instrumentation. Displacement estimates are computed for a reference line of the wing and then evaluated by means of the true non-linear deformation provided by the FE model and estimates of the Modal Rotation Method (MRM, [6, 7]), which has recently been presented as method for application at large displacements of slender structures. The theory of the relevant methods and the framework of this comparative study are explained in the following.

2 MODAL METHODS FOR GEOMETRICALLY NON-LINEAR DEFORMATION

From the various existing displacement reconstruction methods based on strain measurements, both IMM and MRM exploit the modal approach. In the first case, the displacement estimate results directly from linear superposition of displacement mode shapes, whereas the other method superposes curvature modes to rotation angle changes collected in rotation matrices. In order to apply aforementioned methods in an experiment, it is presumed that the structure being analysed is equipped with strain sensors, enabling real-time measurements as the structure experiences deformations either from quasi-static or dynamic loads.

2.1 Incremental Modal Method

For all reconstruction methods based on the modal approach, the structure can be described as a system with N degrees of freedom, where the displacements $\boldsymbol{u}$ can be expressed by means of

a linear combination of mode shapes ϕ_r and modal coordinates q_r:

$$\boldsymbol{u}(t) = \sum_{r=1}^{N} \boldsymbol{\phi}_r q_r(t) = \boldsymbol{\Phi} \boldsymbol{q}(t). \tag{1}$$

$\boldsymbol{\Phi}$ collects the mode shapes in columns being the modal matrix and the components of $\boldsymbol{q}$ indicate the quantitative participation of each mode to the overall deformation. $\boldsymbol{u}$ is an approximation, if $\boldsymbol{\Phi}$ contains a reduced set of modes. Just as the displacements can be described by the modal approach, it is possible to specify strain by a corresponding linear combination:

$$\boldsymbol{\varepsilon}(t) = \sum_{r=1}^{N} \boldsymbol{\psi}_r q_r(t) = \boldsymbol{\Psi} \boldsymbol{q}(t), \tag{2}$$

where $\boldsymbol{\Psi}$ represents likewise the strain modal matrix. The components of $\boldsymbol{\varepsilon}$ are measured during the application of the shape sensing. As the positions for displacement output, for example the position of accelerometers, are in general different from strain sensor locations, the components in $\boldsymbol{\Psi}$ cannot be derived from $\boldsymbol{\Phi}$ in general. But if both the displacement mode shapes and strain mode shapes are scaled with respect to the same modal masses, the modal coordinates are unique and thus the equations can be rearranged to obtain

$$\hat{\boldsymbol{u}}(t) = \boldsymbol{\Phi} \boldsymbol{\Psi}^{\dagger} \boldsymbol{\varepsilon}(t) = \boldsymbol{T} \boldsymbol{\varepsilon}(t) \tag{3}$$

as a displacement estimate. The pseudo-inverse $\boldsymbol{\Psi}^{\dagger}$ of the strain basis functions in combination with the displacement modal matrix can be summarised in a matrix $\boldsymbol{T}$ that conducts the linear mapping from strain to displacement. In view of Eq. (3), the spatial resolution of the displacement estimate depends on the dimension of the displacement mode shape vectors. Their size is either steered by the number of the measurement degrees of freedom in modal testing or the nodal degrees of freedom from FE discretisation. The maximum number of modes considered in the linear combination is typically bounded by the number of strain sensors employed during the test, as they determine how many modes are distinguishable from each other with the chosen strain sensor distribution [11].

Modal matrices can be calculated from finite element analysis or identified in modal testing; also a hybrid combination of modal matrices determined either in tests or from FE analysis is possible. For commercial aircraft, a Ground Vibration Test (GVT) is usually conducted to determine the modal parameters and amongst them mode shapes. The experimentally determined mode shapes represent a favourable basis for shape sensing, because the FE model may underlie flawed modelling assumptions, which are typically corrected in a model update using GVT results. Nevertheless, even mode shapes identified in a GVT or modal test describe the system behaviour under the influence of gravity and thus in a state of insignificant deformation.

Regardless whether the mode shapes are obtained in a test or from a model, in case of geometrically non-linear deformation, the approach described above is limited by the fact that the modal basis is valid for an undeformed structure. Figure 1a illustrates the 1st bending mode of a wing displayed on a reference line. The mode has been determined in a normal modes analysis of an FE model and its shape characterised by components that point exclusively in the z-direction; the same applies for higher order flap-wise bending modes. It is a general property of the modal reconstruction method that deformations due to uniaxial bending loads are compiled with high participation of respective bending modes. Consequently, these mode shapes used as basis functions for deformation reconstruction cannot reproduce any displacement in span-wise direction, which is however typically observed in the geometric non-linear regime.

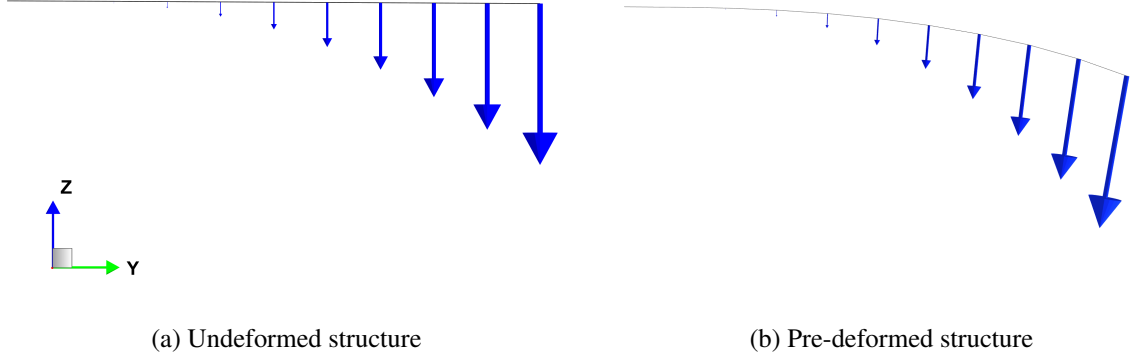(a) Undeformed structure   (b) Pre-deformed structure

Figure 1: 1st flap-wise bending of a wing displayed at the aerodynamic center as reference line. The arrow size corresponds to the magnitude of individual components of the mode shape vector.

With increasing deflection of the wing, the components of individual mode shapes is subjected to changes. In Figure 1b, the 1st bending mode shape is displayed in a deflected state. The mode shape has been obtained from a normal modes analysis following a non-linear static simulation of the wing and it is plotted on the deformed reference line. The eigenvector now exhibits components in y-direction that can contribute to span-wise displacements if the mode is employed in the reconstruction scheme. In an aeroelastic test scenario, sensors that are attached to the wing surface and initially measure in z-direction would be rotated due to the deflection. Consequently, they could also measure span-wise contributions in the mode shapes.

For displacement reconstruction of wing-like structures undergoing large deflections during experiments, a technique is proposed here, where deformations are estimated from one load or deformation increment to the next. During the reconstruction process, the modal basis is adjusted incrementally from one state to another as well, in order to account for changes in the mode shapes attributed to the deformation. The procedure is an analogy to the solution strategy in non-linear FE calculations. If the intermediate states to actually reach a certain state of deformation are the aforementioned quasi-stationary linearisation points that are commonly part of the test envelope, the method would operate model-free solely based on measured data. Based on these considerations, IMM delivers displacement estimates according to:

$$\hat{\boldsymbol{u}}_1 = \boldsymbol{T}_0(\boldsymbol{\varepsilon}_1 - \boldsymbol{0}) = \boldsymbol{T}_0 \boldsymbol{\Delta\varepsilon}_1$$
$$\hat{\boldsymbol{u}}_2 = \boldsymbol{u}_1 + \boldsymbol{T}_1(\boldsymbol{\varepsilon}_2 - \boldsymbol{\varepsilon}_1) = \boldsymbol{u}_1 + \boldsymbol{T}_1 \boldsymbol{\Delta\varepsilon}_2 = \boldsymbol{T}_0 \boldsymbol{\Delta\varepsilon}_1 + \boldsymbol{T}_1 \boldsymbol{\Delta\varepsilon}_2$$
$$\vdots$$
$$\hat{\boldsymbol{u}}_n = \sum_{i=1}^{n} \boldsymbol{T}_{i-1} \boldsymbol{\Delta\varepsilon}_i. \tag{4}$$

In these expressions, ε_i corresponds to the total measured strain after deformation increment i. For a displacement estimation in a presumably geometrically non-linear case, the deformation history is divided into n steps and a modal basis in the form of strain and displacement mode shapes gathered in transformation matrices is required for all previous increments.

2.2 Modal Rotation Method

MRM is a modal method that accounts for large-deformation non-linearity of complex slender structures. The reconstruction principle is based on modal rotations that are derived by modal

analysis of the undeformed FE model. In this research, the non-linear bending behaviour of the investigated wing is described solely in the yz-plane (cf. Figure 1), i.e. the 2D representation of the method is implemented. According to MRM, the structure is segmented along its longitudinal axis in s sections, and the modal matrix consisting of m modes

$$\mathbf{\Phi} = \begin{bmatrix} \phi_{y11} & \cdots & \phi_{y1m} \\ \phi_{z11} & \cdots & \phi_{z1m} \\ \phi_{\theta_{x11}} & \cdots & \phi_{\theta_{x1m}} \\ \vdots & & \vdots \\ \phi_{ys1} & \cdots & \phi_{ysm} \\ \phi_{zs1} & \cdots & \phi_{zsm} \\ \phi_{\theta_{xs1}} & \cdots & \phi_{\theta_{xsm}} \end{bmatrix} \tag{5}$$

specifies the mode shape components of each section. By means of modal curvature κ_x, the changes of the bending rotations $\phi_{\theta x}$ over the segments are

$$\Delta\phi_{\theta_x} = \kappa_x \Delta y = \frac{\partial\phi_{\theta_x}}{\partial y}\Delta y, \tag{6}$$

where Δy corresponds to the length of the segment. Typically a segment is terminated by grid points and the change of bending rotations can directly be assessed as difference of the modal rotations at these locations, for instance

$$\Delta\phi_{\theta_{x11}} = \phi_{\theta_{x11}}^{(e)} - \phi_{\theta_{x11}}^{(s)}, \tag{7}$$

where the superscripts correspond to the start and the end nodes of the segment, respectively. For all segments, the rotation increments can be collected in a modal matrix:

$$\mathbf{\Delta\Phi}_{\theta_x} = \begin{bmatrix} \Delta\phi_{\theta_{x11}} & \cdots & \Delta\phi_{\theta_{x1m}} \\ \vdots & & \vdots \\ \Delta\phi_{\theta_{xs1}} & \cdots & \Delta\phi_{\theta_{xsm}} \end{bmatrix}. \tag{8}$$

It is stated that the curvature and thus the change of rotation angles along the longitudinal axis of the geometric non-linear deformed structure is obtainable by a linear superposition of the gathered modes:

$$\mathbf{\Delta\theta}_x = \mathbf{\Delta\Phi}_{\theta_x}\mathbf{q}. \tag{9}$$

This is the key idea of MRM as, in contrast to displacements, the local curvature and therefore the rotation increments over different segments are kept small if the structure is sufficiently discretised. The corresponding modal coordinates $\mathbf{q}$ in Eq. (9) can be derived by an iterative load correction approach (cf. [6]) or using the strain based modal approach (cf. Eq. (3)); the latter is done in present research according to

$$\mathbf{q} = \mathbf{\Psi}^\dagger \mathbf{\varepsilon}(t). \tag{10}$$

From Eq. (10) it follows that the pseudo-inverse used to calculate the modal coordinates of MRM resembles to the one which is used in IMM in the first deformation increment. The bending rotation increments computed from linear superposition are employed in matrices

$$\mathbf{\Delta R}_j = \begin{bmatrix} \cos\Delta\theta_{x_j} & -\sin\Delta\theta_{x_j} \\ \sin\Delta\theta_{x_j} & \cos\Delta\theta_{x_j} \end{bmatrix} \tag{11}$$

describing the rotation between segments $(j-1)$ and j. From the root of the structure outboard towards the tip, the rotation of a certain segment is obtained via multiplication:

$$\boldsymbol{R}_j = \boldsymbol{R}_{j-1}\boldsymbol{\Delta R}_j. \tag{12}$$

The nodal coordinates $\boldsymbol{x}$ of each segment in the deformed state are calculated by rotation of every segment and summation from the root:

$$\boldsymbol{x}_j = \boldsymbol{x}_{j-1} + \boldsymbol{R}_j\boldsymbol{\Delta l}_j, \tag{13}$$

with

$$\boldsymbol{\Delta l}_j = \boldsymbol{X}_j - \boldsymbol{X}_{j-1} \tag{14}$$

defining the length vector of the j-th segment of the undeformed structure, i.e. the initial configuration. This procedure is comparable to the multi-body system, where the different segments are connected to each other via rotational degrees of freedom. Finally, the estimated displacement vector can be resolved according to

$$\hat{\boldsymbol{u}} = \boldsymbol{x} - \boldsymbol{X}. \tag{15}$$

In contrast to IMM, the displacement estimate computed with MRM does not rely on updating of mode shapes over the deformation history. The results are however constraint to the reference line in which the modal rotations are defined.

3 CASE OF APPLICATION

The reconstruction methods described above are applied to the FE model of a high aspect ratio wing with symmetric cross-sections. The wing has a swept and tapered design; in comparison with conventional laboratory structures such as straight beams and flat plates it therefore exhibits properties that commonly impair the accuracy of the displacement reconstruction. In the following, the properties of the model and the simulation setup are presented before reconstruction results of a specific bending load case are discussed.

3.1 Model properties

The laboratory model of the wing consists of shells and shear webs built from sandwich-structured composites as well as ribs that stiffen the cross-sections at regular intervals. The dimensions of the geometry are summarised in Table 1. The geometry is discretised with 8949 elements, by the majority with 4-noded shell quadrilaterals associated with composite properties specifying the laminate lay-up. The FE model has been created with the DLR-AE in-house parametric model generator ModGen [12] in MSC.NASTRAN. A top view of the model is displayed in Figure 2. As the laboratory wing is being built for multiple purpose, it contains a folding wing tip, which is not of relevance for this investigation. The hinge of the wing tip is visible as a gap of $0.1\,\mathrm{m}$ at two-thirds of the wing span. The connection over the hinge is

Table 1: Wing parameters.

Parameter	Value
half span	$5\,\mathrm{m}$
planform area	$3\,\mathrm{m}^2$
aspect ratio	16.67
sweep angle	$29°$

modelled entirely rigid in the shape sensing analysis.

From the mesh, one can recognise the location of virtual strain sensors for the representation of strain mode shapes and for in-situ strain information during the deformation history used to compute modal coordinates as stated in Eq. (10). Strain is assessed in 5 cross-sections on shell panels that are connected with the leading and trailing edge, respectively. The instrumented sections start at $y = 0.75\,\mathrm{m}$ with equidistant increments of $1\,\mathrm{m}$ in-between. The orientation of the collected strain corresponds to the first axis of the elementary coordinate system, which lies in the direction of the local sweep. Both the pressure and suction side of the wing are instrumented at locations symmetric to the xy-plane. In total, 20 virtual strain channels are thus available; a similar distribution of strain sensors could be used to evaluate bending moments as part of a load monitoring of the wing [13].
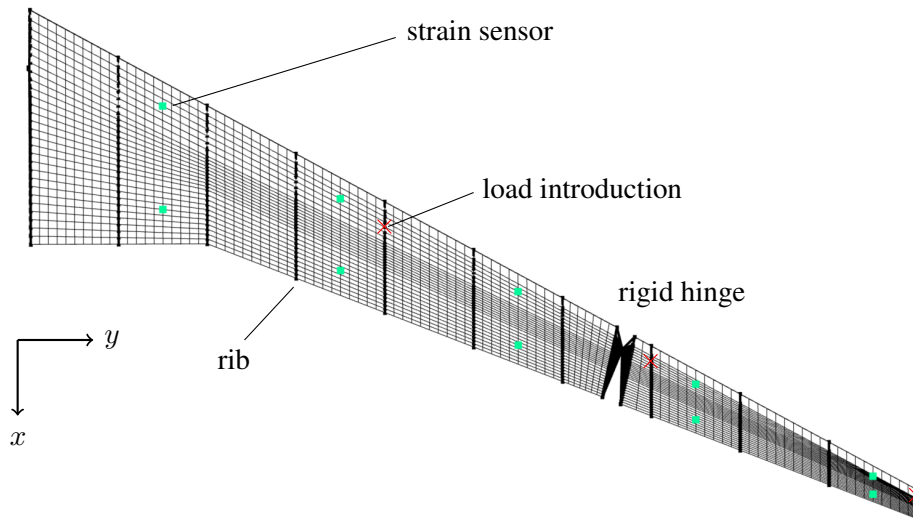

Figure 2: Finite element model of the investigated wing. The positions of virtual strain sensors are indicated on the shell panels. In steps of $.5\,\mathrm{m}$, ribs stiffen the cross-sections. The incontinuity at about two-thirds of the wing length is rigidly modelled.

The shape sensing methods presented in section 2 are compared in a geometrically non-linear state which is determined by means of a NASTRAN SOL400 static simulation. For this purpose, the wing model is clamped at the root and, as indicated in the mesh plot, forces are introduced as point loads in the aerodynamic center (i.e. quarter chord) of three cross-sections at $2\,\mathrm{m}$, $3.5\,\mathrm{m}$, and $5\,\mathrm{m}$. At these locations forces of equal amplitude are applied as dead loads, that is in negative z-direction irrespective of the instantaneous deformation of the structure. The load introductions points on the reference line are connected to the nodes on the shell contour via RBE2 rigid body constraints. Above described setup is selected, because it represents a conceivable structural test scenario rather than being physical meaningful with regard to the pressure distribution of aerodynamic loading. This approach is considered as appropriate, as the primary aim is to evaluate the displacement reconstruction while the cause of the deformation is of minor relevance.

3.2 Reconstruction results

In the course of the non-linear FE calculation, the applied forces and therefore the deflection of the wing increase. A load case producing a tip deflection of up to $23\,\%$ with respect to the half wing span is considered in the following. The deformation of the structure leads to changes in the modal parameters, i.e. both the eigenfrequencies and the eigenvectors. This is illustrated in Figure 3 for the first ten modes whose denotation is listed in Figure 3c with ascending fre-
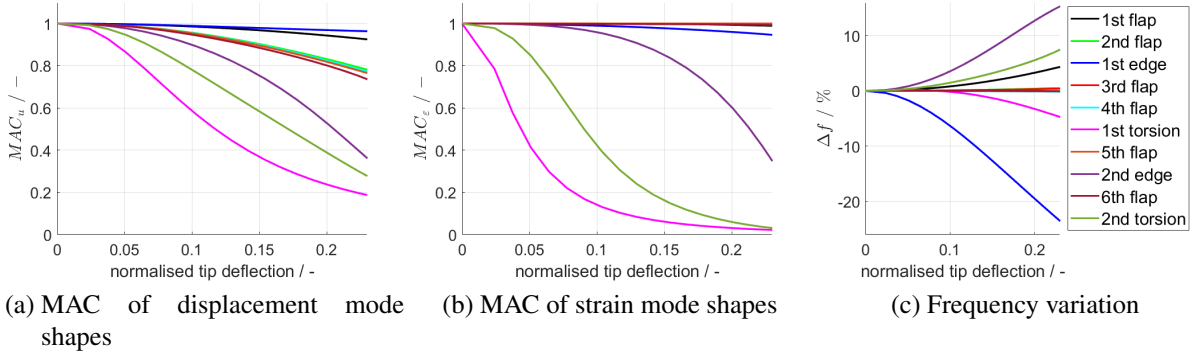
(a) MAC of displacement mode shapes

(b) MAC of strain mode shapes

(c) Frequency variation

Figure 3: MAC values of mode shapes and related frequency changes with respect to the undeformed state for increasing bending deflection in z-direction.

quency. Due to the deformation, eigenfrequency changes of more than $20\,\%$ can be expected; edge-wise and torsion modes are particularly susceptible, which has also been observed for other wing designs (cf. [14]).

In order to assess the change of mode shapes with increasing deflection, the Modal Assurance Criterion (MAC) with respect to the eigenvectors of the undeformed structure is evaluated. MAC values crucially depend on the sensor positions and degrees of freedom taken into account [15]. In order to calculate the displacement MAC, the translational degrees of freedom in the quarter chord points are considered at equidistant intervals of $10\,\%$ relative wing length. Regarding the strain MAC, the strain mode shapes consist of components from the 20 virtual strain sensors as depicted in Figure 2. In terms of the MAC, collinear modes indicate a value of 1 and orthogonal modes exhibit a value of 0. From both MAC comparison plots (Figures 3a and 3b) one can observe that the torsion modes and the 2nd edge-wise bending mode are subjected to severe changes. The strain mode shapes of the torsion modes exhibit a particularly steep gradient even below $10\,\%$ tip deflection. The modes that are most relevant for the deformation reconstruction, namely the flap-wise bending modes, show however comparatively slight changes. In this context, it should be noted that MAC represents a global measure to compare eigenvectors. For this reason, local alterations of the mode shapes towards the tip of the wing, as indicated in Fig. 1b, may only lead to minor changes in the MAC value. Overall, the diagrams indicate that the mode shapes undergo significant changes with increasing deformation. This necessarily leads to changes in the modal coordinates (Eq. 10) and therefore transformation matrices (Eq. 4), which can be accounted for through the application of IMM.

3.2.1 Modal basis of the undeformed model

In principle, displacement estimates can be provided using the modal basis of the undeformed structures even in cases of large displacements. As a starting point, this is accomplished for different fractions of the total load and compared to the non-linear FE results in Figure 4. The curves show the deflection of the wing in the yz-plane evaluated in the aforementioned quarter chord points. The strain and displacement eigenvectors of the first ten modes are considered in the reconstruction.

From the diagrams in Figure 4a one can observe a good agreement for lower force levels corresponding to a tip deflection below $10\,\%$ semi-span; a greater deviation between the estimate $\hat{u}$ and the true FE result u is however indicated for increasing deflection of the wing. A uniform characteristic of all estimates is the fact that no displacements in span-wise direction are included. This is an inherent feature of the reconstruction using mode shapes of the undeformed
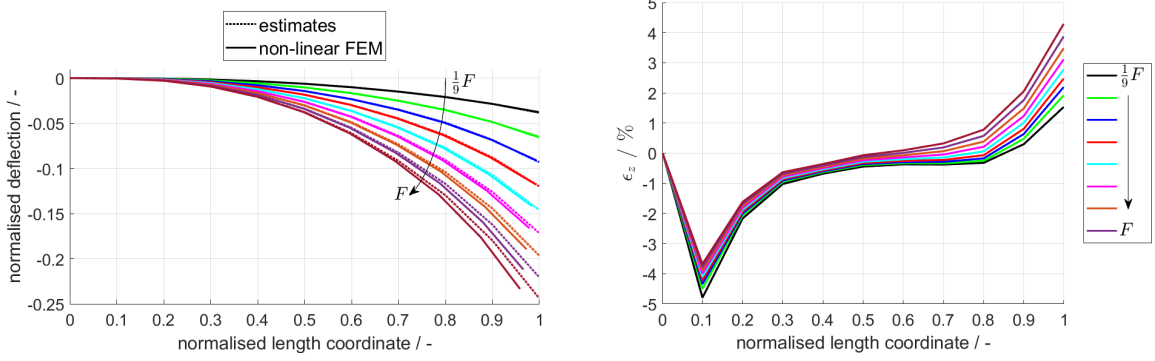
(a) Deflection curves: estimates vs. non-linear FEM results

(b) Error of displacement in z-direction along span

Figure 4: Bending deflection estimates from modal method using mode shapes of undeformed wing in comparison with FEA for different load states.

structure as they do not contain span-wise motion (cf. Fig. 1a). In Figure 4b the relative error

$$\epsilon_z = \frac{\hat{u}_z - u_z}{u_z} \tag{16}$$

is depicted. An assessment of the displacement error in y-direction is not meaningful as no displacement in this direction is predicted by the shape sensing method. It should be noted that the graphs are drawn with respect to the initial configuration of concerning nodes. For this reason, towards the wing tip the error yields $\epsilon_z > 0$, although the deflection curves of the estimates show a lower deflection compared to the FE curve.

3.2.2 Incremental reconstruction

In order to demonstrate the suitability of IMM for geometrically non-linear deformed structures, the load case with the largest deflection is reconstructed with a different number of increments and compared with MRM. For the latter, it is assumed that modal rotations are available at the nodes of ten segments going through the aerodynamic center of the wing. This represents a comparatively small number of segments which could possibly be realised by using inertial measurement units in an experiment. For the application of IMM, the accelerometers are situated at the very same location. In Figure 5 the comparison of the methods is shown. Again, the first ten mode shapes are used as the modal basis. The modal method using a modal basis of the initial configuration is also considered meaning the number of increments to the full load is equal to $n = 1$. For all the other cases, the total load is divided in equidistant force increments and the mode shapes are determined after each step as required by Eq. (4). From the global deflection curves one can tell that all estimates run fairly close to the non-linear FE solution. A more informative view is obtained from Fig. 5b, where a close-up of the curves at the wing tip is shown. Here, a non-monotonic convergence can be observed as the differences of the IMM solutions at the tip amongst each other decrease with higher number of increments. A higher number of increments does however not necessarily lead to convergence towards the numerical FE results. The MRM solution lies in the tip region in-between the range of IMM results.

As soon as intermediate states are considered in IMM, span-wise displacements are predicted. As a consequence, the solution accuracy significantly improves. Figure 6 describes how the relative displacement errors change with an increasing number of increments until the final state of deformation is reached. Analogous to the error in bending deflection, the relative error of

(a) Deflection curves from incremental procedure
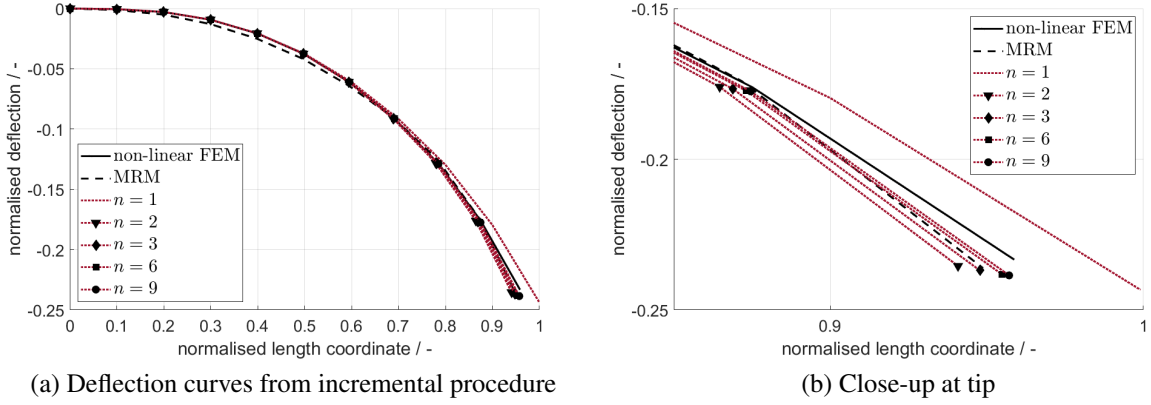
(b) Close-up at tip

Figure 5: Deflection estimates from incremental modal method in comparison with modal rotation method.

displacements in span-direction is defined by

$$\epsilon_y = \frac{\hat{u}_y - u_y}{u_y}. \tag{17}$$

For both methods ϵ_y is one magnitude larger compared to ϵ_z. Applying IMM, ϵ_y is nearly constant along the wing span. Accuracy can be gained by increasing the number of increments; using $n = 9$ increments closely approximates the true FE result. Regarding ϵ_z, increasing n leads eventually to a converged path, as evidenced from the curves of $n = 6$ and $n = 9$, which nearly lie on top of each other. The curves from IMM qualitatively resemble to the graphs in Fig. 4b, even though the modal basis is changed on the way to the final displacement estimate. A higher number of increments does however not necessarily produce the most accurate estimate, which is particularly recognisable at the tip. This behavior is admissible, as the superposition of mode shapes already exhibits an error in linear problems. This error should be distinguished from inaccuracies caused by an insufficient number of increments.

The MRM estimate is most inaccurate towards the root, and both errors curves exhibit the similarity of a global minimum at the same position of 0.8 relative half span. This is possibly due to the rotation of the segments that steer displacements in both directions.

Reconstruction results of shape sensing schemes that depend on a modal basis are in general influenced by the number and the shape of the considered modes participating in the linear superposition. For the investigated problem, this relationship is illustrated in Figure 7. The plots
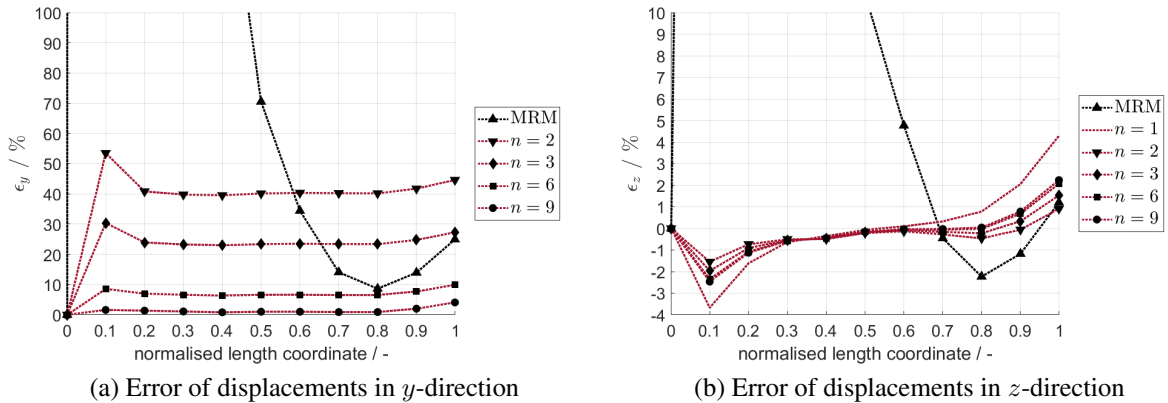

(a) Error of displacements in y-direction

(b) Error of displacements in z-direction

Figure 6: Relative displacement error along span with respect to the undeformed state.

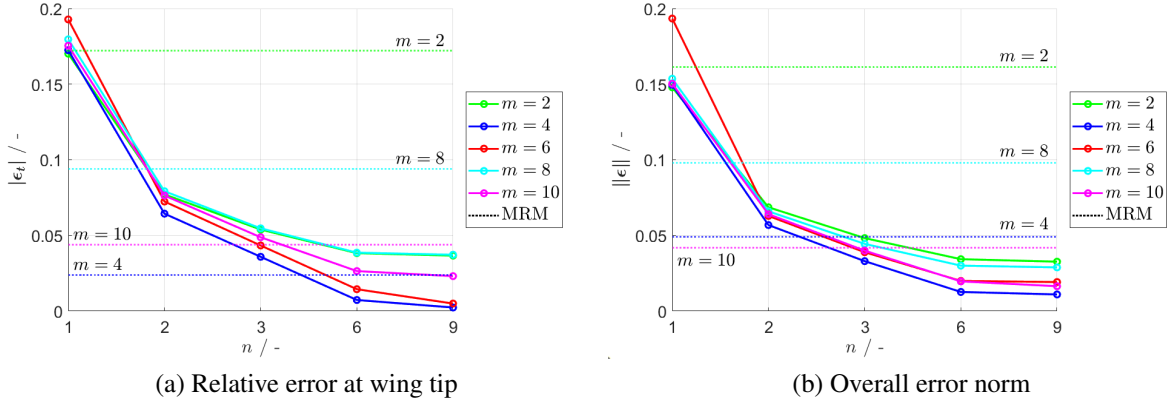(a) Relative error at wing tip (b) Overall error norm

Figure 7: Relative displacement error displayed for different amount of mode shapes considered in the approximation.

can be interpreted as a sort of convergence study of the number of modes m and the number of increments n required to obtain a certain accuracy. The tip displacement error specified with

$$\boldsymbol{\epsilon}_t = \frac{1}{|\boldsymbol{u}_t|} \begin{bmatrix} \hat{u}_{y,t} - u_{y,t} \\ \hat{u}_{z,t} - u_{z,t} \end{bmatrix} = \frac{\boldsymbol{\Delta u}_t}{|\boldsymbol{u}_t|} \tag{18}$$

is outlined in Figure 7a (cf. Fig. 3c for order of modes). Since the modal rotation method is likewise affected by changes in the choice of mode shapes, its results are presented in dashed lines as well. The diagrams point out that an increase in increments in the scope of IMM leads to an improvement of the accuracy at the tip irrespective of the number of modes considered. Furthermore, for this rather simple uni-axial load case, a higher number of modes does not necessarily lead to greater accuracy, as the kinematics of the deformation is likely covered by a few flap-wise modes. In the setup presented with only ten segments, MRM turns out to be more sensitive regarding the subsets of modes used for the reconstruction. In case of $m = 6$ modes, the error at the tip happens to be exceptionally high with a value larger than 1. There is moreover for all mode combinations a threshold of increments where IMM yields more accurate estimates.

A similar picture emerges when considering an error norm

$$\|\boldsymbol{\epsilon}\| = \frac{\left| [|\boldsymbol{\Delta u}_1|, \ldots, |\boldsymbol{\Delta u}_t|]^T \right|}{\left| [|\boldsymbol{u}_1|, \ldots, |\boldsymbol{u}_t|]^T \right|} \tag{19}$$

that is defined over the entire wing length. Corresponding curves are depicted in Figure 7b. The graphs indicate that the tip error is already a well-suited measure for the global performance of the shape sensing methods applied.

4 CONCLUSION

In this research, the Incremental Modal Method (IMM) is introduced and applied to the reconstruction of wing displacements under geometric non-linear bending deformations. The study demonstrates that conventional modal reconstruction, which assumes linear deformation, fails to provide accurate displacement estimates. By taking into account the changes in mode shapes due to structural deformations, the IMM offers a promising alternative. Simulation results of the FE model, equipped with virtual strain sensors, indicate that IMM can accurately track the deformation of the wing throughout its load history. This is accomplished by updating the modal

11

basis at each deformation increment. When compared to the Modal Rotation Method (MRM), IMM shows superior performance if the total deformations is subdivided in sufficient number of increments. Moreover, IMM appears to be less sensitive to the composition of the modal basis. The findings suggest that IMM can be effectively implemented in experimental setups with appropriate strain sensor instrumentation, enhancing the accuracy of displacement reconstruction for flexible aerospace structures. Several aspects require further investigation before practical application of IMM can be realised in test campaigns. Key areas for future research include noise analysis and the propagation of this uncertainty to the displacement estimates. This topic is also related to the robustness of the method with respect to sensor failure or distribution of employed strain sensors. More complicated load cases must be evaluated to assess the performance of IMM under a wider range of load conditions, in particular with focus on torsion deformation. Overall, future work will focus on addressing these challenges to enhance the robustness and applicability of IMM, before the method is validated on the laboratory wing in an experiment.

5 ACKNOWLEDGEMENT

Supported by:

Federal Ministry
for Economic Affairs
and Climate Action

on the basis of a decision
by the German Bundestag

6 REFERENCES

[1] Ko, W. L., Richards, W. L., and Tran, V. T. (2007). Displacement theories for in-flight deformed shape predictions of aerospace structures. Tech. rep., NASA/TP-2007-214612.

[2] Gherlone, M., Cerracchio, P., and Mattone, M. (2018). Shape sensing methods: Review and experimental comparison on a wing-shaped plate. *Progress in Aerospace Science*, 99, 14–26. doi:10.1016/j.paerosci.2018.04.001.

[3] Bogert, P. B., Haugse, E. D., and Gehrki, R. E. Structural shape identification from experimental strains using a modal transformation technique.

[4] Glaser, R., Caccese, V., and Shahinpoor, M. (2012). Shape monitoring of a beam structure from measured strain or curvature. *Experimental Mechanics*, 6, 591–606.

[5] Cesnik, C. E. S., Senatore, P. J., Su, W., et al. (2012). X-hale: A very flexible unmanned aerial vehicle for nonlinear aeroelastic tests. *AIAA Journal*, 50, 2820–2833. doi:10.2514/1.J051392.

[6] Drachinsky, A. and Raveh, D. E. (2020). Modal rotations: A modal-based method for large structural deformations of slender bodies. *AIAA Journal*, 58(7), 3159–3173.

[7] Drachinsky, A. and Raveh, D. E. (2022). Nonlinear aeroelastic analysis of highly flexible wings using the modal rotation method. *AIAA Journal*, 60(5), 3122–3134.

[8] Pak, C.-G. (2023). Linear and geometrically nonlinear structural shape sensing from strain data. *AIAA Journal*, 61(2). doi:10.2514/1.J062165.

[9] Böswald, M., Govers, Y., Jelicic, G., et al. Online monitoring of flutter stability during wind tunnel testing of an elastic wing with pylon and engine nacelle within the hmae1 project.

[10] Tessler, A., Roy, R., Esposito, M., et al. (2018). Shape sensing of plate and shell structures undergoing large displacements using the inverse finite element method. *Shock and Vibration*. doi:10.1155/2018/8076085.

[11] Foss, G. C. and Haugse, E. D. Using modal test results to develop strain to displacement transformation.

[12] Klimmek, T. (2009). Parameterization of topology and geometry for the multidisciplinary optimization of wing structures. In *Proceedings of the European Air and Space Conference 2009*.

[13] Schmücker, M. (2010). *LTH - Aeronautical Engineering Handbook: Calibration of Main Components of an Aircraft for Loads*. Ottobrunn: LTH Executive Secretary.

[14] Hilger, J. and Ritter, M. (2021). Nonlinear aeroelastic simulations and stability analysis of the pazy wing aeroelastic benchmark. *Aerospace*, 8(308). doi:10.3390/aerospace8100308.

[15] Allemang, R. J. (2003). The modal assurance criterion – twenty years of use and abuse,. *Sound and Vibration*, 14–20.

COPYRIGHT STATEMENT